Semester Project - Advanced NEMS Laboratory

Characterization of Suspended Piezoelectrically Transduced Resonators

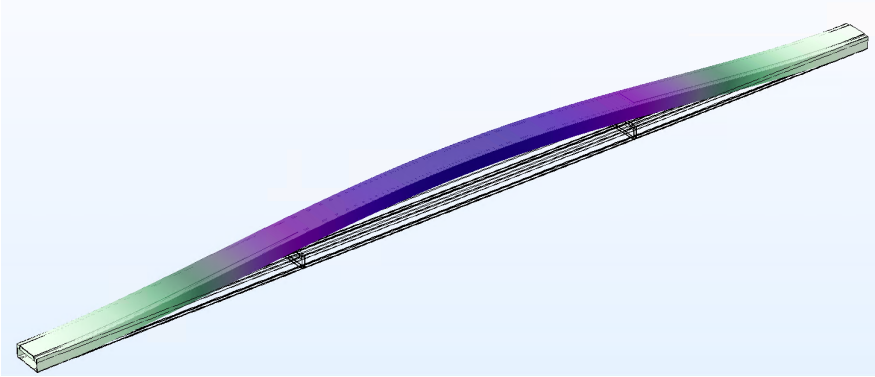

by

Ehret Maxime

for

Prof. Villanueva Guillermo, Maillard Damien and Abdelaal Yara

Abstract

This report presents the characterization of singly-clamped and doubly-clamped resonator devices.
Resistance tests were performed to ensure adequate top-to-bottom insulation, allowing the characterization work to proceed. The piezoelectric characteristics of the devices were evaluated through their transverse piezoelectric coefficient, d_{31}.
In order to estimate this coefficient in singly-clamped devices, the resonators were driven at resonance with increasing drive voltages and their behaviour was compared to the theory.
In doubly-clamped devices, the method consisted in applying a DC bias through the piezoelectric layer, which modulated the stress within the resonator and thus altered the resonance frequency. The d_{31} could then be extracted after thorough matching with simulations.

Contents

1 Introduction

1.1 Goal of the study

The objective of this semester project is to determine the value of the transverse piezoelectric coefficient, d_{31}, of suspended piezoelectrically transduced beam resonators. This coefficient gives the induced in-plane strain per unit electric field applied perpendicularly to the film plane. The resonators were made by another student in a previous semestre project. Twelve wafers were then made. They were essentially similar in terms of the devices that they contained, they only varied on some small aspects. For instance one some wafers, the top electrode was made out of titanium and on some others of aluminum nitride. The thickness of the platinum layer also varied from one wafer to the next. Some wafers were made using lift-off, others reflow. The deposition for some wafers was made at room temperature and for others at high temperature. The piezoelectric layer of these devices was composed of aluminum scandium nitride 17% (AlSc0.17N).

These devices are ultimately meant to be used to characterize molecules properties. Those molecules would pass through channels placed on the resonators. The devices must thus be able to detect very subtle frequency variations : this is where the d_{31} coefficient comes into play. Indeed, the d_{31} describes how big an electric charge is induced by a given strain applied to a piezoelectric material. A material with great detection properties will generate a large charge for a small strain, it will thus have a large d_{31} coefficient, whose unit is C per N.

1.2 Characterization methods

Two types of resonators are considered : singly-clamped and doubly-clamped. This is important to note because the method used to characterize the d_{31} will change based on the type of resonator.
For the singly-clamped devices, the coefficient is determined by measuring the relation between the amplitude of oscillation of the tip of the beam and the actuation voltage. Probes are placed on the electrodes of the measured device. A voltage is applied through them to drive the resonator at its resonance frequency.
The change in stress in the doubly beam when actuated with a given voltage is used to find the d_{31}.

2 Devices and preliminary tests

2.1 Devices description

As mentioned before, two types of resonators are studied : singly- and doubly-clamped. This section aims at presenting both of them.

Singly-clamped

The first type of resonator is a cantilever with a clamped end and a free one. As descibed in Figure 1, the device is composed of four main parts : a silicon nitride (Si3N4) base, the bottom electrode with a base of aluminum (Al) or titanium (Ti) and a layer of platinum (Pt), the piezoelectric layer made of aluminium scandium nitride (AlScN) and finally the top electrode made out of aluminum. The devices are actuated by imposing an electrical potential between the two electrodes, which would actuate the piezoelectric layer. The devices have five different lengths : 50 μm, 100 μm, 150 μm, 200 μm and 250 μm (see Figure 2).

Figure 1: Cross-section view of the design of the singly-clamped devices

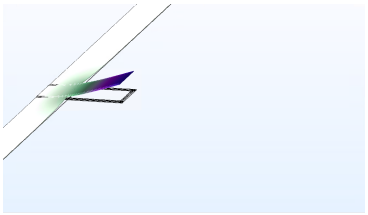

(a) 50 μm

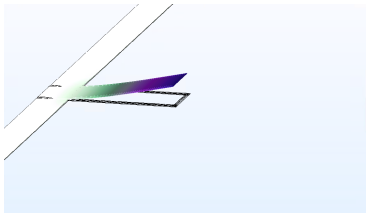

(b) 100 μm

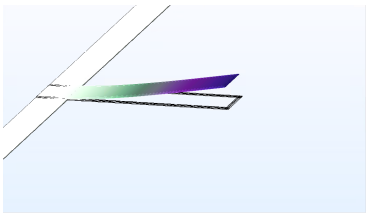

(c) 150 μm

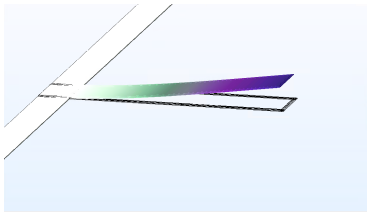

(d) 200 μm

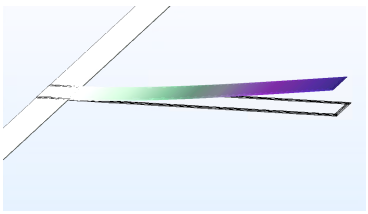

(e) 250 μm

Figure 2: Simulations of the singly-clamped resonators

Doubly-clamped

The second type of resonator is doubly-clamped chanelled beams. Their design is fairly similar to that of the singly-clamped devices described above : a silicon nitride base, a platinum bottom electrode, a piezoelectric layer made out of either aluminium scandium nitride or aluminum nitride (AlN) and a platinum top electrode, see Figure 3. The actuation is done just like for the singly-clamped resonators. The main difference between doubly- and singly-clamped devices (apart from the clamping system) is that there was a channel inside

the silicon base in the doubly-clamped ones. Those devices have two nominal lengths : 250 μm and 500 μm (see Figure 4).

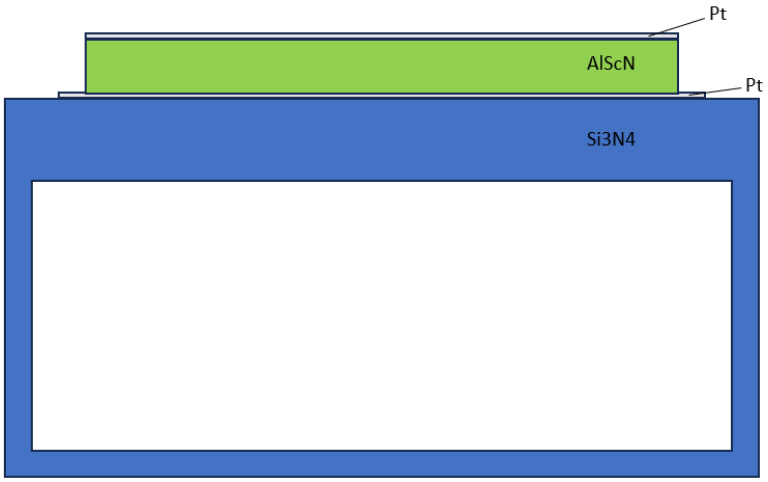

Figure 3: Cross-section view of the design of the doubly-clamped devices

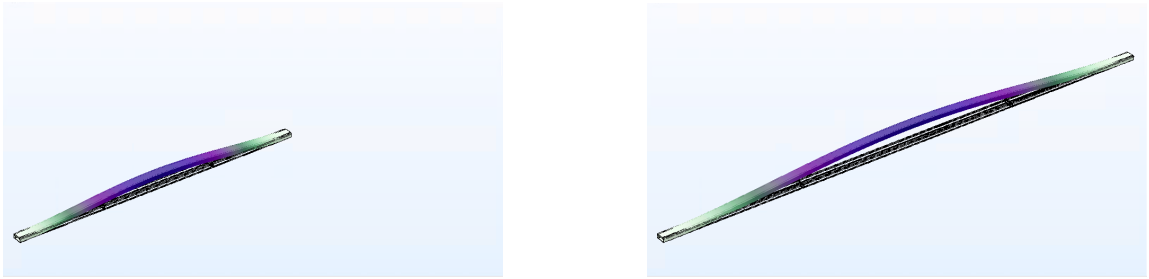

(a) 250 μm (b) 500 μm

Figure 4: Simulations of the doubly-clamped resonators

2.2 Resistance tests

Before starting the characterization themselves, some preliminary tests were necessary. As mentioned above, each device is composed of two or three electrodes. Before going any further, it was necessary to ensure that the devices had a correct top-to-bottom insulation. That's why the first thing that was done were the resistance tests. Each electrode of the resonator is connected to a pad, every device had thus two or three pads. When the devices have two pads, one is connected to the bottom electrode and the other to the top one. In the devices with three pads, one is for the bottom electrode and two for the top one ; one of the top electrodes is meant to be used for actuation and the other for detection. During the measures, the two probes of the measuring stations are placed on the pads and the resistance between them is measured. There were six possible configurations for the measurements (see Table 1). About fourty measures were performed on randomly chosen devices for each of the twelve wafers. When the probes were placed on the same pad (Figure 5a), the resistance was

low and when they were one separate pads (Figure 5b), the resistance was very high, this meant that there were no shortcuts between the layers of the devices : the characterization work could begin.

Probe 1	Probe 2	Combination
A	A	A-A
A	G	A-G
A	D	A-D
G	G	G-G
G	D	G-D
D	D	D-D

Table 1: Six possible types of measures for the probe station (A : Actuation pad, G : Ground pad, D : Detection pad)

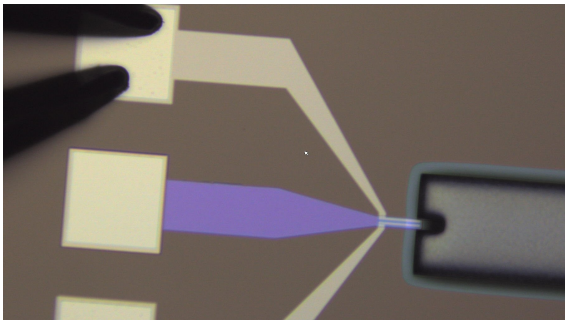

(a) Resistance test on actuation pad (A-A)

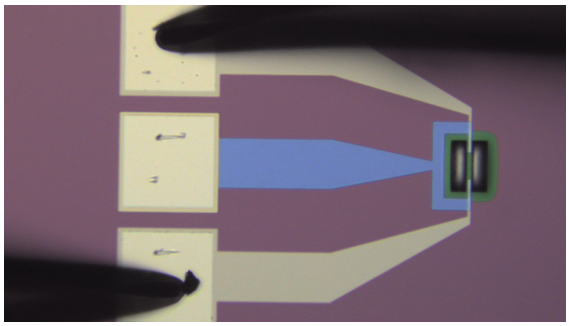

(b) Resistance test on actuation and detection pads (A-D)

Figure 5: Two resistance tests

3 Characterization of singly-clamped devices

As mentioned before, the d_{31} of the singly-clamepd beams is determined using the relation between the actuation voltage and the amplitude of the tip of the device. This section presents in details the method followed to extract the d_{31} of the devices from the measures, the measures performed, the results themselves and finally a discussion about them.

3.1 Method and measurements

Simulations

The first step is the determination of the d_{31} coefficient is the simulation of the beams using the software COMSOL. These simulations give the theoretical resonance frequencies of the devices that are required in the next steps of the characterzation. The simulations are made for two heights of the platinum layer : 25 and 50 μm. To give an idea of the impact of the thickness of the piezoelectric layer on the resonance frequency, the simulations were made for

four different thicknesses : 180, 200, 220 and 240 μm. It was observed that the piezoelectric thicknesses for which the frequencies best matched the observations were 200 and 220 μm. The simulated frequencies are given in Table 2 for the devices with a platinium layer of 25 nm and Table 3 for those with a 50 nm layer. As can be observed on those tables, the thicker the piezoelectric layer, the higher the resonance frequency. Indeed, when the thickness increases, so does the stiffness of the resonator, resulting in a higher resonance frequency.

	Frequency (Hz)			
Nominal length (μm)	piezo height : 180 μm	piezo height : 200 μm	piezo height : 220 μm	piezo height : 240 μm
50	1,89E+05	1,94E+05	1,99E+05	2,04E+05
100	6,78E+04	6,97E+04	7,16E+04	7,34E+04
150	3,42E+04	3,52E+04	3,62E+04	3,72E+04
200	2,06E+04	2,12E+04	2,18E+04	2,24E+04
250	1,37E+04	1,41E+04	1,45E+04	1,49E+04

Table 2: Simulated frequencies of singly-clamped devices with a platinum layer of 25 nm for different heights of the piezoelectrical layer

	Frequency (Hz)			
Nominal Length (μm)	piezo height 180 μm	piezo height 200 μm	piezo height 220 μm	piezo height 240 μm
50	1,82E+05	1,87E+05	1,91E+05	1,96E+05
100	6,52E+04	6,71E+04	6,90E+04	7,09E+04
150	3,30E+04	3,40E+04	3,50E+04	3,59E+04
200	1,98E+04	2,04E+04	2,10E+04	2,16E+04
250	1,32E+04	1,36E+04	1,40E+04	1,44E+04

Table 3: Simulated frequencies of singly-clamped devices with a platinum layer of 50 nm for different heights of the piezoelectrical layer

Measurements using the Laser Doppler Vibrometry station

The devices are measured using the Laser Doppler Vibrometry (LDV) station. Firstly the resonance frequency is determined as well as the thermomechanical noise (see Figure 6). Once this is done, the device is driven using two probes placed on the electrode pads with different voltages. the amplitude of the resonator at resonance frequency is observed for each of those voltages. As the actuation voltage is increased the amplitude of the device gets larger and larger (see Figure 7). Three voltages were applied on each device: 0.5, 1 and 1.5 V.

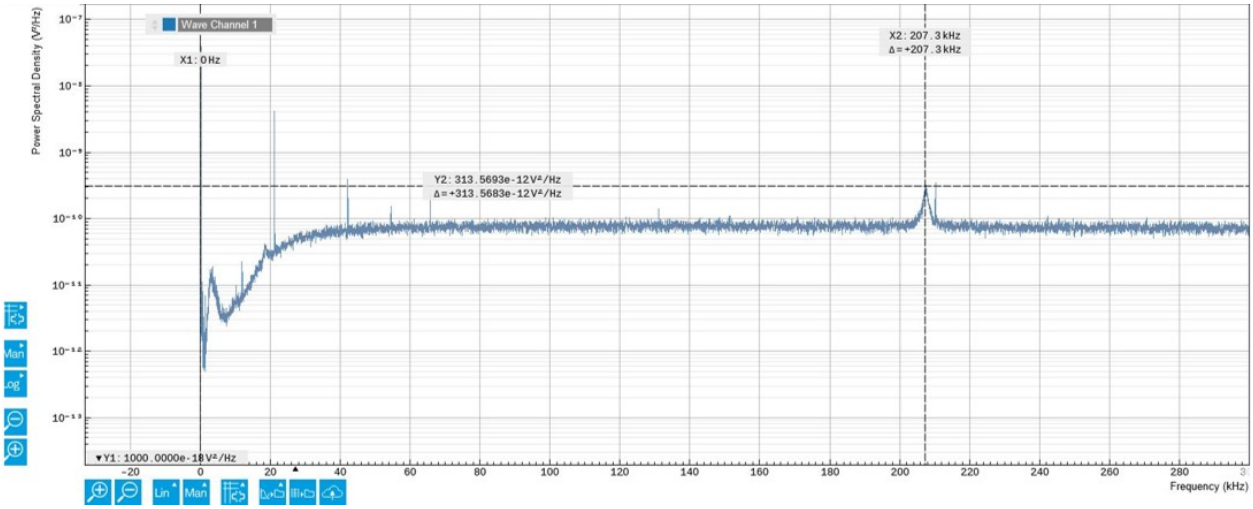

Figure 6: Frequency scope of a 50 μm singly-clamped resonator

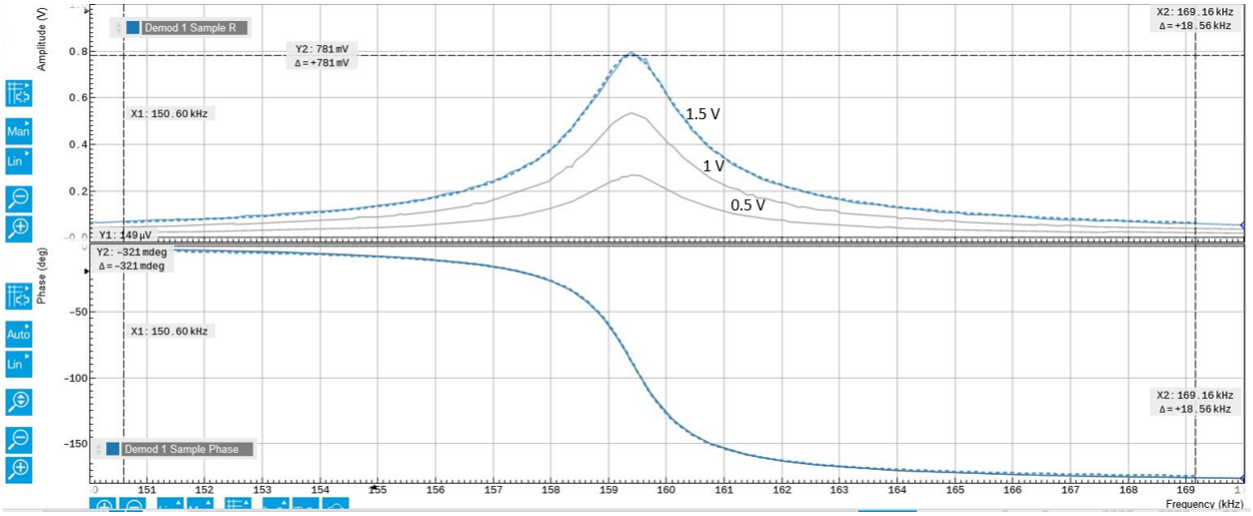

Figure 7: Bode plot of a 50 μm singly-clamped resonator

What is of interest here was the amplitude at the tip of the devices, since the formulas used to determine the d_{31} are based on the amplitude at the extremity of the beam. However, the laser beam of the LDV cannot be placed exactly at the tip : the amplitude ploted on Figure 7 is thus the amplitude somewhere on the beam, where the laser is pointed at. To palliate the issue, a correction factor R is introduced.
It is defined as :

$$R = \frac{TMN_{exp}}{TMN_{th}} \tag{1}$$

Where TMN_{exp} is the experimental thermomechanical noise measured by the LDV and TMN_{th} the theoretical thermomechanical noise, given by :

$$TMN_{th} = \frac{k_B T Q}{2\pi^3 m_{eff} f_0^3} \tag{2}$$

With :

- $k_B = 1.3806e^{-23}\ m^2kgs^{-2}K^{-1}$ the Boltzmann constant
- T the ambient temperature
- Q the quality factor of the device (determined using the LDV)
- m_{eff} the effective mass of the device
- f_0 the resonance frequency of the device

The amplitude at the tip u_{tip} is calculated from the amplitude at the position where the laser beam is placed u as :

$$u_{tip} = \sqrt{\frac{2}{R}}u \tag{3}$$

The $\sqrt{2}$ factor is used to correct the measure considering the crest factor.

It is now possible to plot the maximal amplitude of the device as a function of the actuation voltage, as shown on Figure 8. There seems to be a linear relation between the two values; the slope of the tendency line will be useful for the next step.

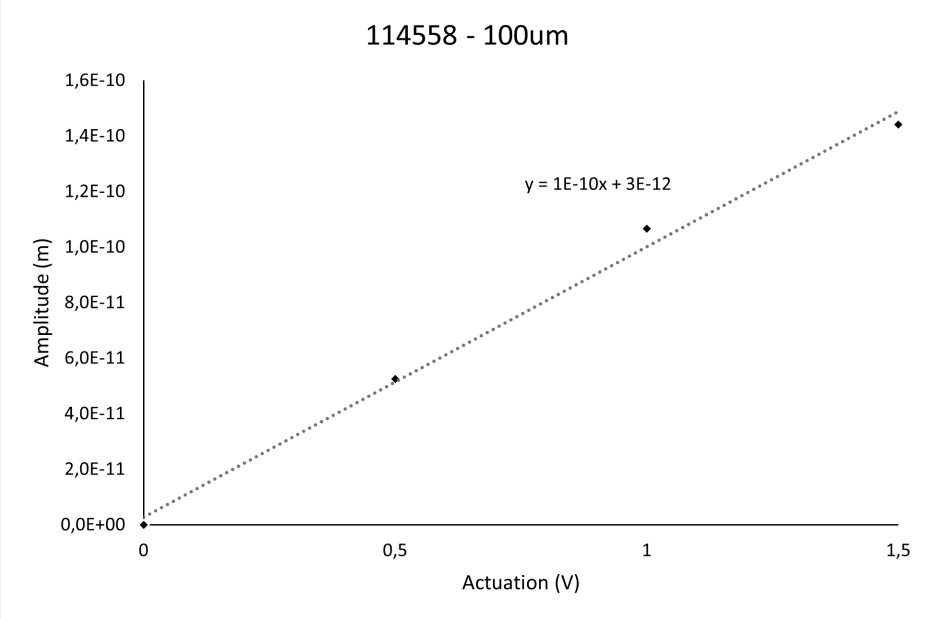

Figure 8: Amplitude of the tip of the device at resonance frequency as a function of the actuation voltage for a singly-clamped device of 100 μm

Numerical calculation

Once all of the aforementioned measures are done, all that is left to do is the numerical calculation of the d_{31} coefficient itself.

Let's firstly note that according to the theory, the displacement at the tip of the cantilever is given by :

$$u_n(\omega) = \chi_n^A \frac{d_{31} z_{offset} L^2}{t_{total}^3} \frac{V}{1 - (\frac{\omega}{\omega_0})^2 + j\frac{\omega}{\omega_0} Q} \frac{w_{elec}}{w_{canti}} \tag{4}$$

Where :

- u_n the displacement at the tip
- ω the driving frequency
- ω_0 the resonance frequency
- $\chi_n^A = 1.38$ for for cantilever with full length electrodes
- d_{31} the transverse piezoelectric coefficient
- $z_{offset} = t_{total} - z_0$ the off-axis placement of the PZE layer with respect to the neutral axis
- t_{total} the total thickness of the resonator
- $z_0 = \frac{\sum E_i t_i z_i}{\sum E_i t_i}$ the neutral axis
- L the length of the resonator
- V the driving voltage
- Q the quality factor of the resonator
- w_{elec} the width of the electrode
- w_{canti} the width of the resonator

At resonance frequency, Equation 4 becomes :

$$u_n(\omega = \omega_0) = \chi_n^A \frac{d_{31} z_{offset} L^2}{t_{total}^3} \frac{V}{jQ} \frac{w_{elec}}{w_{canti}} \tag{5}$$

Isolating the d_{31} term yields :

$$d_{31} \approx \frac{t_{total}^3}{\chi_n^A z_{offset} L^2 Q} \frac{w_{canti}}{w_{elec}} slope \tag{6}$$

With $slope = \frac{u_n(\omega)}{V}$ the slope of the maximal amplitude as a function of the actuation voltage.

3.2 Results and discussion

Using Equation 3.1 introduced above, the d_{31} coefficients of some devices with AlScN as their piezoelectric material were calculated. The results are gathered in Table 4. It appeared that the values found are much lower than expected. Indeed, the d_{31} of AlScN is supposed to be around $10^{-12}C/N$, the values calculated are between $10^{-18}C/N$ and $10^{-16}C/N$.

Device	d_{31} (C/N)
114403 - 50 μm	1.61 E-16
114403 - 100 μm	1.06 E-18
114558 - 50 μm	1.74 E-16
114558 - 100 μm	1.04 E-16
114559 - 100 μm	9.35 E-17
114608 - 50 μm	5.30 E-16
114608 - 100 μm	2.28 E-16

Table 4: Calculated d_{31} coefficients of seven singly-clamped devices

To see if there was a problem in the calculation, the d_{31} of two test devices, that were known to have a d_{31} of about $10^{-12}C/N$, was determined. The devices also had an AlScN piezoelectric layer and a 25 μm thick platinum layer. The results are given in Table 5 and prove to be much closer to the expected values as the first ones. The calculation method was thus not the cause of the wrong values.

Device	d_{31} (C/N)
Test - 50 μm	1.23 E-13
Test - 100 μm	5.09 E-13

Table 5: Calculated d_{31} coefficients of two singly-clamped test devices

Further examinations of the wafers was performed and it turned out that there was a problem in their fabrication, causing a short circuit. This meant that they could no longer be used for the rest of the project. The measurements on the doubly-clamped devices would thus be performed on some other devices that were properly fabricated.

4 Characterization of doubly-clamped devices

Due to a problem in the fabrication of the wafers, the doubly-clamped devices made last semester could not be characterized. Instead, four doubly-clamped devices, correctly fabricated are studied. The piezoelectric layer of two of them is made of AlScN and that of the two remaining is of AlN. For each material, one device is 250 μm long and the other 500 μm. This section describes the way the d_{31} of those devices is determined.

4.1 Method and measurements

Unlike what was done with the singly-clamped devices, the d_{31} coefficient of doubly-clamped devices is not done numerically. Rather it is determined using its amplitude when actuated

at resonance frequency. Indeed, because the beams are constrained on both ends, the oscillation amplitude of those devices is much smaller. When an actuation is applied, the stress within the beam changes however. This modification in the stress causes a shift in frequency that will be more or less important depending on the d_{31} of the device.

The d_{31} would thus be determined by observing the frequency shift occurring when an actuation bias is applied and finding the value of the coefficient that would produce such a shift.

Frequency measurements with the LDV

Using the LDV station, the resonance frequency of the devices is found. They are then actuated with different DC biases : -1, -0.5, 0, 0.5 and 1 V. A change in frequency is observed when a non-zero bias is applied, which created the steps that can be observed on Figure 9.

It could be observed that the graphs giving the frequency of the shorter devices (250 μm) are rather noisy, especially that of AlN, which would lead to more uncertainty in the results. A second observation is that for the AlScN, when the bias is negative, the frequency increases and when positive it decreases ; whereas for the AlN, it is the opposite : with a negative bias, the frequency is lower than with zero bias and when the bias is positive, the frequency increases. This is very unexpected and possibly due to an inversion of the probes that would cause an inversion of the sign of the bias to occur. This would later be corrected by inverting the relevent values of the biases for the measures on the AlN devices. The different frequencies measured and the frequency shifts (considering the frequency when no bias is applied as the reference one) are respectively given by Table 6 and Table 7.

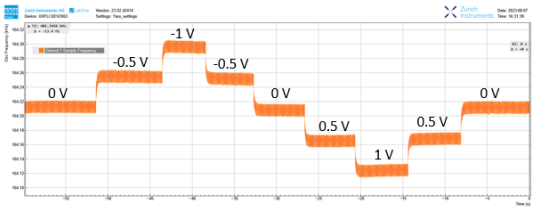

(a) AlScN 500 μm

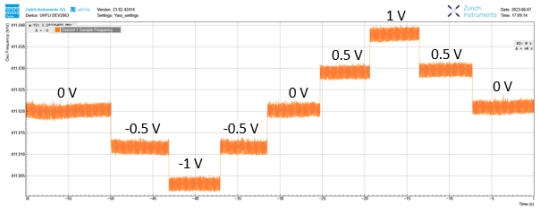

(b) AlN 500 μm

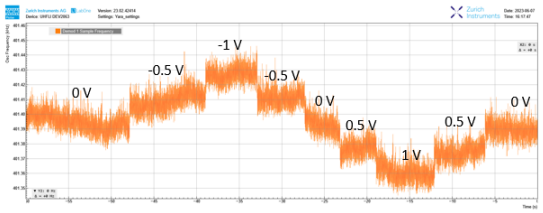

(c) AlScN 250 μm

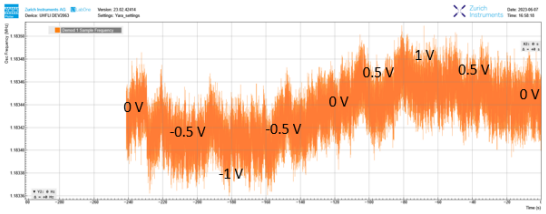

(d) AlN 250 μm

Figure 9: Frequency shift of clampled-clamped devices when the DC bias changes

	Frequency (kHz)			
DC bias (V)	AlScN - 250μm	AlScN - 500μm	AlN - 250μm	AlN - 500μm
-1	401,4294	164,2962	1183,3976	411,0035
-0.5	401,4108	164,2545	1183,4136	411,0117
0	401,3925	164,2115	1183,4372	411,0201
0.5	401,3745	164,1663	1183,4594	411,0292
1	401,3590	164,1242	1183,4718	411,0379

Table 6: Measured frequencies of the doubly-clamped devices for different DC biases

	Frequency shift (ppm)			
DC bias (V)	AlScN - 250μm	AlScN - 500μm	AlN - 250μm	AlN - 500μm
-1	-91,9300	-515,7982	33,4619	40,3873
-0.5	-45,5913	-261,8574	19,9419	20,4370
0	0	0	0	0
0.5	44,8439	275,2548	-18,7589	-22,1400
1	83,4595	531,6315	-29,2369	-43,3069

Table 7: Frequency shifts of the doubly-clamped devices for different DC biases (let's note that on this graph the sign of the frequency shifts of the AlN devices have not yet been inverted)

Simulated frequency shifts

The second part in the determination of the d_{31} was the simulation of the frequency shifts of the devices using COMSOL.

Firstly, the devices were constructed on the software. It was important to make sure that the simulated beams had a resonance frequency close to the ones that were measured with the LDV station. This was done by adjusting the initial stress in the beams as summarized in Table 8. It appears that to have matching frequencies between the experiments and the simulations, the pre-stress imposed on the 250 μm devices of both materials must be very negative. In the case of the AlScN devices, there is a difference of 225 MPa in the initial stress between the 250 μm and 500 μm devices. For the AlN, this difference is goes as high as 430 MPa ! It is really unlikely that the stress changes that much between two devices that are so close on the same chip. There is a massive discrepancy whose origin is unknown and this probably doesn't represent the actual behaviour of the beams.

Device	Initial stress (MPa)
AlScN - 250 μm	-220
AlScN - 500 μm	5
AlN - 250 μm	-270
AlN - 500 μm	160

Table 8: Initial stress in the simulated doubly-clamped beams

The same DC biases as in the measurements were applied to the simulated beams and the induced frequency shifts were recorded. This process was repeated for several values of d_{31}. Once the simulations were done for a large range of d_{31}, it was possible to compare the experimental results with the theoretical ones to find an approximation for the value of the coefficient for the devices.

4.2 Results and discussion

Following the method described previously, the frequency shifts of each devices for a DC bias between -1 V and 1 V were simulated with COMSOL for ten values of d_{31} between -1E-12 and -1E-11 C/N. For each device, the simulated shifts and the measured ones were plotted on a graph, see Figure 10 and Figure 11. Based on where the experimental values were placed on the graph (black dots on Figure 10 and Figure 11), it was simple to estimate the d_{31} for a given device, the estimated d_{31} coefficient for each of them is given on Table 9.

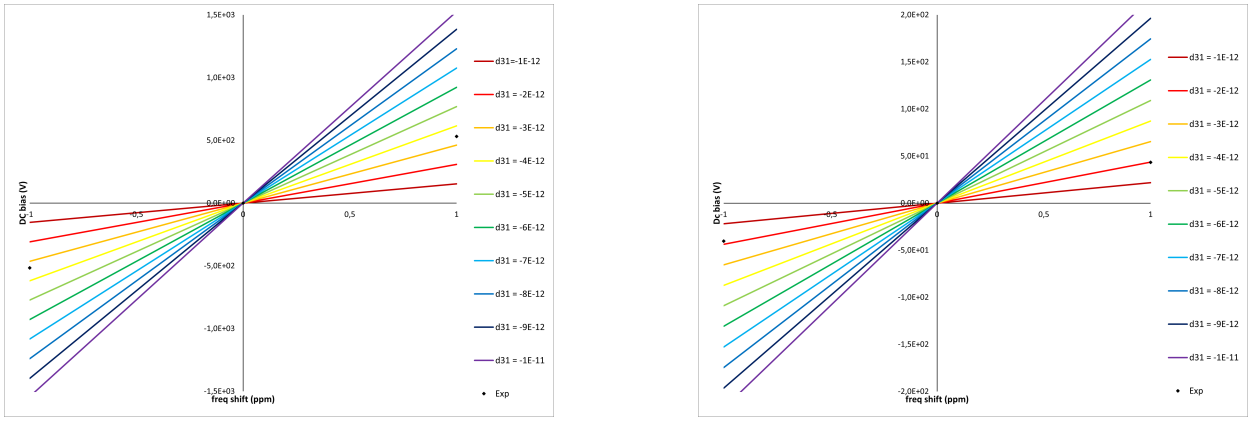

(a) AlScN 500 μm

(b) AlN 500 μm

Figure 10: Frequency shift of clampled-clamped 500 μm devices when the DC bias changes (See Table 10)

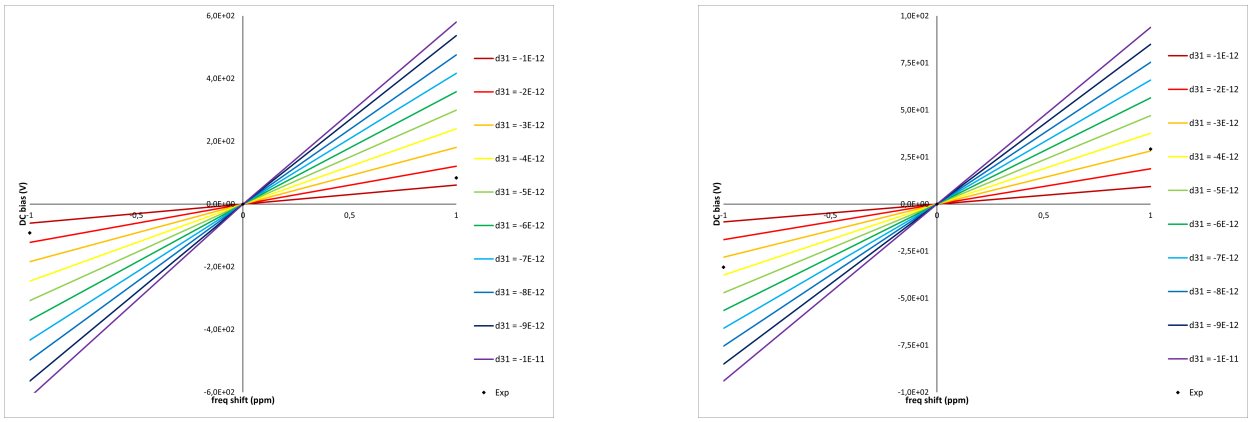

(a) AlScN 250 μm

(b) AlN 250 μm

Figure 11: Frequency shift of clampled-clamped 250 μm devices when the DC bias changes (See Table 10)

Device	d_{31} (C/N)
AlScN - 250μm	-1.5E-12
AlScN - 500μm	-3.5E-12
AlN - 250μm	-3E-12
AlN - 500μm	-2E-12

Table 9: Estimated d_{31} coefficient of the doubly-clamped devices

The d_{31} of the clamped-clamped devices are in accordance with the theory since they are around 10^{-12} C/N. However these results must be nuanced. Indeed, as discussed previously, the measures made on the 250 μm devices had a lot of noise and more importantly, the pre-stress that had to be imposed in the simulations is unlikely to accurately describe the reality. Those are potential sources of error. As a result, to have more conclusive results, more measurements would have to be performed in the future with more devices, a wider range of lengths and perhaps even a different combination of materials.

5 Conclusion

In conclusion, this characterization work devices proved to be challenging for the singly-clamped devices but also produced the expected results for the doubly-clamped ones. The singly-clamped devices exhibited d_{31} coefficients much lower than expected, indicating fabrication issues that rendered them unusable for the project. Further examination of the wafers confirmed the presence of short circuits. In contrast, the d_{31} values for the doubly-clamped devices were within the theoretical range. However, the noisy frequency measurements and unlikely pre-constrained state of the devices added complexity to the analysis. Overall, these

findings emphasize the importance of thorough fabrication quality control and highlight the need for additional investigations to accurately determine the d_{31} coefficient of the devices.

ANNEX

		250 um AlScN		250 um AlN		500 um AlScN		500 um AlN	
d31 (C/N)	DC bias (V)	Frequency (Hz)	Frequency shift (ppm)	Frequency (Hz)	Frequency shift (ppm)	Frequency (Hz)	Frequency shift (ppm)	Frequency (Hz)	Frequency shift (ppm)
	-1	401668,245833117	-60,80145667	1185871,36020676	-9,40301286	177722,532459209	-154,0785895	413288,836006909	-21,78075143
-1,00E-12	0	401643,825303476	0	1185860,20954796	0	177695,153440598	0	413279,834461563	0
	1	401619,562627504	60,40843763	1185849,06245516	9,40000576	177667,792849098	153,9748888	413270,837632588	21,76933938
	-1	401693,205111321	-122,0271305	1185882,54790114	-18,82153185	177750,024408024	-308,5593121	413297,854028925	-43,59598111
-2,00E-12	0	401644,193622879	0	1185860,22819508	0	177695,194900924	0	413279,836688973	0
	1	401595,741758957	120,6337965	1185837,90688968	18,82288053	177640,453781464	308,0619006	413261,821373205	43,59108325
	-1	401718,604846406	-183,6607011	1185893,75377668	-28,24789899	177777,601780797	-463,4404252	413306,867630500	-65,4093857
-3,00E-12	0	401644,838473787	0	1185860,25571596	0	177695,250618287	0	413279,835250356	0
	1	401572,329761120	180,5294273	1185826,77255191	28,23533708	177613,162671114	461,9591513	413252,817865798	65,37310136
	-1	401744,571484077	-245,5965461	1185904,97728540	-37,66875958	177805,202177848	-618,2083743	413315,885866061	-87,23189254
-4,00E-12	0	401645,928631239	0	1185860,30739859	0	177695,349424767	0	413279,834683932	0
	1	401549,486305356	240,1177729	1185815,65518124	37,65385946	177585,936120892	615,7353258	413243,808647318	87,17104874
	-1	401771,352636911	-307,9928589	1185916,23582655	-47,09727677	177832,937299320	-773,1486262	413324,898126414	-109,0404403
-5,00E-12	0	401647,648029512	0	1185860,38503179	0	177695,552227231	0	413279,833911346	0
	1	401527,413834249	299,3524196	1185804,56394187	47,07222758	177558,810376456	769,5288321	413234,788401579	108,9951797
	-1	401799,432800676	-370,6806658	1185927,54865036	-56,52190124	177860,812273601	-928,27939	413333,911026675	-130,8452265
-6,00E-12	0	401650,548707858	0	1185860,52155907	0	177695,860868264	0	413279,835333025	0
	1	401506,617870990	358,3484134	1185793,53156884	56,49061505	177531,812420367	923,197913	413225,781893211	130,7913796
	-1	401830,250255638	-433,9216353	1185938,99292478	-65,95969079	177888,999918185	-1083,533741	413342,928272860	-152,7052483
-7,00E-12	0	401655,963043322	0	1185860,77391481	0	177696,459808257	0	413279,818275584	0
	1	401488,448060528	417,0608635	1185782,60842482	65,91455904	177505,135345365	1076,692598	413216,760520229	152,5788402
	-1	401869,137469003	-497,7767143	1185950,82164516	-75,40782569	177918,139085343	-1239,657524	413351,945561148	-174,5625812
-8,00E-12	0	401669,195896443	0	1185861,39841553	0	177697,854602888	0	413279,802372068	0
	1	401478,071357482	475,8257315	1185772,04410277	75,34971024	177479,291879248	1229,968275	413207,721126420	174,4126987
	-1	401970,985278462	-564,3044694	1185965,87975395	-84,97738518	177954,496960025	-1396,99009	413360,968231869	-196,5412207
-9,00E-12	0	401744,279186156	0	1185865,10803789	0	177706,243099427	0	413279,741726924	0
	1	401528,613484770	536,8233291	1185764,43550997	84,89374317	177460,095812087	1385,135846	413198,583834056	196,3752023
	-1	401765,521861667	-615,5601741	1185967,45371820	-94,04055294	177958,737511725	-1541,67731	413370,179497190	-217,8498252
-1,00E-11	0	401518,363148144	0	1185855,93517035	0	177684,804879721	0	413280,146489537	0
	1	401285,325346250	580,3913925	1185744,53863167	93,93766593	177413,595003558	1526,353795	413190,203821711	217,6312329

Table 10: simulated frequencies and deduced frequency shifts for the four devices for ten values of d_{31}